Received: 28 January 2021 | Accepted: 25 February 2021

DOI: 10.1002/mmce.22623

RESEARCH ARTICLE

INTERNATIONAL JOURNAL OF RF AND MICROWAVE COMPUTER-AIDED ENGINEERING WILEY

A magnetic-free in-band full-duplex RF front-end with antenna balancing structure

Junhyung Jeong[1] | **Girdhari Chaudhary**[2] | **Yongchae Jeong**[2]

[1]IT Application Research Center, Jeonbuk Regional Branch, Korea Electronics Technology Institute, Jeonju, South Korea

[2]Division of Electronics and Information Engineering, IT Convergence Research Center, Jeonbuk National University, Jeonju-si, South Korea

Correspondence
Yongchae Jeong, Division of Electronics and Information Engineering, IT Convergence Research Center, Jeonbuk National University, Jeonju-si 54896, South Korea.
Email: ycjeong@jbnu.ac.kr

Funding information
National Research Foundation of Korea, Grant/Award Number: 2020R1A2C2012057; National Research Foundation, Grant/Award Number: 2016H1D3A1938065

Abstract

In this article, a design of magnetic-free in-band full-duplex (IBFD) RF front-end with antenna balancing structure is presented. The proposed magnetic-free IBFD RF front-end consists of 3 dB hybrid couplers, a Wilkinson power divider, two transmitter (Tx) antennas, and two receiver (Rx) antennas. The proposed IBFD RF front-end can be implemented and integrated at high frequencies because all the components used in the circuit are non-magnetic devices. Proposed IBFD RF front-end eliminated the 3-dB Tx insertion-loss of the Balun and transformer in conventional IBFD RF front-ends using antenna balancing structure. Moreover, there is no noise figure degradation at Rx because it realized only a passive circuit. The mathematical analysis of the cancellation characteristics between two different signals with magnitude and phase difference variations according to the normalized frequencies is presented. Accordingly, the broadband out-of-phase balancing power splitter and the antenna balancing structure are adopted to achieve broadband SIC. In order to verify the electrical performances of the proposed magnetic-free IBFD RF front-end, it was implemented at the 2.5 GHz WiMax frequency band. When the fabricated IBFD RF front-end was operated with antenna balancing structure, the measurement results show that the 60 dB SIC bandwidth and maximum SIC were 113 MHz (2.446 - 2.559 GHz) and 75.6 dB, respectively.

KEYWORDS

analog cancelation, antenna balancing, balanced structure, balancing power splitter, in-band full-duplex circuit, magnetic-free, wideband self-interference cancellation (SIC)

1 | INTRODUCTION

After the practical results of the in-band full-duplex (IBFD) system[1,2] were first reported, various approaches to realize IBFD systems have been explored.[3-15] Compared with the conventional frequency division duplex, the IBFD has a double frequency spectrum efficiency, because it simultaneously transmits and receives signals on the same frequency. As transmitter and receiver use the same frequency, some portion of strong transmitting (Tx) signals is leaked to the receiving (Rx) port and serves as a type of self-interference. Although only a very small portion of Tx signals is leaked into the Rx port, these signals can seriously interfere with Rx signals due to the relatively strong Tx signal power. Therefore, the required isolation between the Tx and Rx ports for the proper operation of the IBFD system has been studied and reported in Reference 1. The required isolation of IBFD depends on the leaked Tx power in the Rx and noise floor of the Rx, but a minimum of 110 dB isolation is generally

required for the overall IBFD system from Reference 1. Particularly in the RF stage, isolation of 60 dB or more should be achieved to protect Rx. When Tx leakage in Rx of the RF front-end does not suppress sufficiently, Rx cannot operate due to the saturation of the low noise amplifier by leakage of Tx.

The self-interference cancellation (SIC) technique is mainly used in order to obtain at least 60 dB isolation between Tx and Rx in the RF stage. The SIC techniques can be classified into antenna SIC and RF front-end SIC. When SIC is applied to an antenna, high isolation characteristics can be easily obtained by using the proper physical structures of the antenna.[16-18] However, the antenna SIC needs to use a specific antenna, which is not suitable for application to an array antennas system, and more than 60 dB isolation can only be obtained over the narrow frequency band. RF front-end SIC can also achieve isolation of more than 60 dB over the narrower band, but various kinds of antennas are available. In the cases of SIC circuits using magnetic device such as a circulator, it is easy to isolate the Tx and Rx ports with a single antenna.[16] However, high isolation cannot be obtained by using magnetic devices alone, and other supplementary signal cancellation techniques must be used. Moreover, as the operating frequency increases, the isolation characteristic of magnetic devices is degraded and becomes difficult to integrate with other circuits. Without magnetic devices, realizing 60 dB isolation over a wide bandwidth is difficult. The works[19-22] show the RF front-end SIC circuits without magnetic devices. In Reference 19, the magnetic device replaced the hybrid balun and transformer. However, the half (3 dB) of Tx power is lost because a half of the output signal power in the balun or transformer is used as the cancellation signal in the Rx port. It is possible to obtain a Tx and Rx isolation characteristic without the 3 dB Tx loss by using multiple antennas with antenna diversity technique.[21] However, it is difficult to implement antenna diversity in the broadband and the isolation bandwidth is not sufficient. In Reference 22, a balanced structure was used to enhance the isolation bandwidth. However, the 60 dB isolation bandwidth was only 60 MHz, and it had the aforementioned drawbacks due to the use of a circulator.

In this article, a magnetic-free IBFD RF front-end with wide bandwidth SIC capability is presented. In order to overcome the drawbacks of previous works, the proposed novel IBFD RF front-end adopts broadband out-of-phase balancing power splitter (BPS) and antenna balanced structure. Analytical design equations are derived to analyze the SIC characteristics according to the leakage signals pairs in the proposed balance. For validation, the experimental results of the novel magnetic-free IBFD RF front-end are provided.

2 | MATHEMATICAL ANALYSIS

Figure 1 shows the proposed magnetic-free IBFD RF front-end consisting of 3 dB hybrid couplers, Wilkinson power divider/combiner, and antennas. The proposed IBFD RF front-end adopts a balanced structure (symmetric up and down) and out-of-phase BPS for broadband SIC.[23] All Tx signals are transmitted through two Tx antennas after 0°/180° conversion using out-of-phase BPS. However, the signals received from two Rx antennas are in-phase combined at the Rx port. Therefore, it does not have any 3 dB loss, which is a basic problem of the conventional IBFD RF front-ends using a 3 dB hybrid Balun and transformer. Moreover, there is no noise figure degradation at Rx by active circuit because it uses only a passive circuit.

Figure 2 shows schematics of out-of-phase BPS and the reflective signal transmitter. The out-of-phase BPS consists of a 3 dB Wilkinson power divider and two reflective signal transmitters. The input signal is divided into two output signals with the same magnitude, group delay, and phase by 3 dB Wilkinson power divider. These two divided signals pass through the reflective signal transmitter of Figure 2B with open and shorted load Z_L, respectively. The S-parameters of reflective signal transmitter in Figure 2(B) is derived as Equation (1) using the port reduction method.[23] The transmission coefficient (S_{21}) of reflective signal transmitter is controlled by the reflection coefficient Γ_L.

$$S_{RST} = \begin{bmatrix} 0 & -j\Gamma_L \\ -j\Gamma_L & 0 \end{bmatrix}, \tag{1}$$

equation (2) shows the Γ_L according to termination impedance Z_L. According to the open and short conditions, the Γ_L can have the same magnitude and different signs. Therefore, the proposed out-of-phase BPS has a

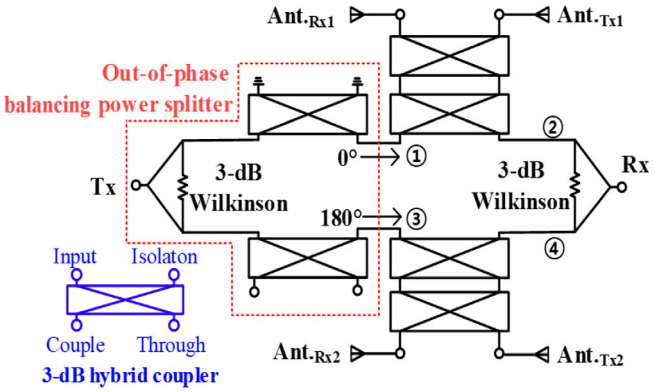

FIGURE 1 Proposed magnetic-free in-band full-duplex circuit

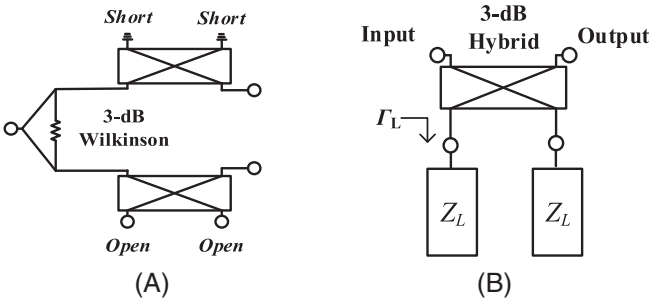

FIGURE 2 A, Out-of-phase balancing power splitter and B, reflective signal transmitter

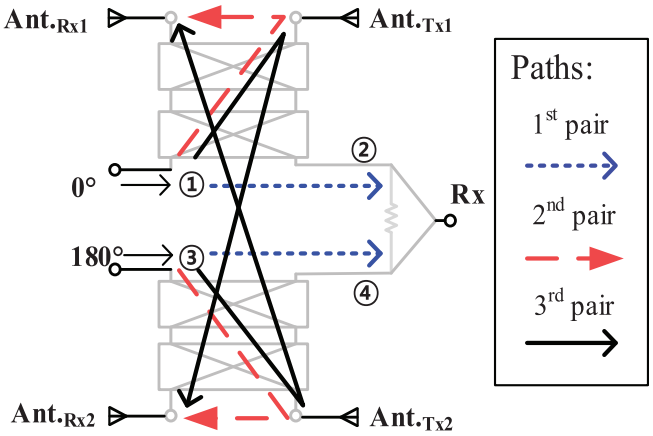

FIGURE 3 Paths of leakage transmitter (Tx) signal pairs in proposed magnetic-free in-band full-duplex circuit

180° phase difference between the two output signals with the same magnitude and group delay.

$$\Gamma_{L\_shrot} = \left.\frac{Z_L - Z_0}{Z_L + Z_0}\right|_{Z_L=0} = -1, \tag{2a}$$

$$\Gamma_{L\_open} = \left.\frac{Z_L - Z_0}{Z_L + Z_0}\right|_{Z_L=\infty} = 1, \tag{2b}$$

due to the balanced structure of the proposed IBFD RF front-end, there are pairs of Tx leakage signals into the Rx port. Figure 3 shows the paths of Tx leakage signal pairs in the proposed IBFD RF front-end. The first pair signals are $S_{leak\_H\_up}(t, f)$ and $S_{leak\_H\_down}(t, f)$, which through the 3 dB hybrid couplers due to the non-ideal isolation characteristic of the hybrid. The second and third leakage pair signals are $S_{leak\_T1R1}(t, f)$, $S_{leak\_T2R2}(t, f)$ and $S_{leak\_T1R2}(t, f)$, $S_{leak\_T2R1}(t, f)$, respectively, which are caused by cross-coupling among the Tx and Rx antennas. Table 1 shows the leakage signal names and their detailed paths. Each leakage pair signals with the same

TABLE 1 Leakage pairs and paths in proposed IBFD RF front-end

	Names	Paths
First Pair	$S_{leak\_H\_up}(t,f)$	①-②
	$S_{leak\_H\_down}(t,f)$	③-④
Second Pair	$S_{leak\_T1R1}(t,f)$	①-Ant.$_{Tx1}$-Ant.$_{Rx1}$-②
	$S_{leak\_T2R2}(t,f)$	③-Ant.$_{Tx2}$-Ant.$_{Rx2}$-④
Third Pair	$S_{leak\_T1R2}(t,f)$	①-Ant.$_{Tx1}$-Ant.$_{Rx2}$-④
	$S_{leak\_T2R1}(t,f)$	③-Ant.$_{Tx2}$-Ant.$_{Rx1}$-②

Abbreviation: IBDF, in-band full-duplex.

magnitude and phase variations depending on time and frequency can cancel each other out at the Rx port due to the dividing characteristic of out-of-phase BPS. Therefore, the mathematical model can be used to analyze the SIC characteristics of the proposed IBFD RF front-end according to the characteristics of these leakage signal pairs.

The dependence of the leakage signal with time and frequency can be defined as shown in Equations (3) and (4).

$$\begin{aligned} S_{leak}(t,f) &= Aa(f)\cos(2\pi f(t-\tau)+\varphi+\theta(f)) \\ &= Aa(f)\left\{\begin{array}{l}\cos(2\pi ft)\cos(\varphi+\theta(f)-2\pi f\tau) \\ -\sin(2\pi ft)\sin(\varphi+\theta(f)-2\pi f\tau)\end{array}\right\} \\ &= Aa(f)(B\cos(2\pi ft)-C\sin(2\pi ft)), \end{aligned} \tag{3}$$

where

$$B = \cos(\varphi+\theta(f)-2\pi f\tau), \tag{4a}$$

$$C = \sin(\varphi+\theta(f)-2\pi f\tau), \tag{4b}$$

A, $a(f)$, $\theta(f)$, φ, and τ are the magnitude, magnitude variation function along frequency, phase variation function along frequency, reference phase and group delay of the signal, respectively.

Leakage pair signals are combined at the Rx port which can be expressed as Equation (5) using (3).

$$\begin{aligned} S_{Rx}(t,f) &= S_{leak1}(t,f) + S_{leak2}(t,f) \\ &= \cos(2\pi ft)[A_1B_1a_1(f)+A_2B_2a_2(f)] \\ &\quad -\sin(2\pi ft)[A_1C_1a_1(f)+A_2C_2a_2(f)], \end{aligned} \tag{5}$$

the leakage pair signals of $S_{leak1}(t, f)$ and $S_{leak2}(t, f)$ mutually have a 180° phase difference as well as the same τ_0 because of the out-of-phase BPS and physical balanced

structure of the proposed IBFD RF front-end. To analyze SIC characteristics of the proposed structure, the small magnitude and phase difference between two leakage signals are as described below.

$$A_2 = \Delta m + A_1, \tag{6}$$

$$\varphi_2 = \pi + \Delta p + \varphi_1, \tag{7}$$

$$\tau_1 = \tau_2 = \tau_0, \tag{8}$$

where Δm and Δp are the magnitude and phase differences between $S_{leak1}(t, f)$ and $S_{leak2}(t, f)$, respectively. Using the above conditions, Equation (5) can be written as shown below.

$$\begin{aligned} S_{Rx}(t,f) = &\cos(2\pi ft)\{A_1B_1a_1(f) + (\Delta m + A_1)B_2a_2(f)\} \\ &-\sin(2\pi ft)\{A_1C_1a_1(f) + (\Delta m + A_1)C_2a_2(f)\}, \end{aligned} \tag{9}$$

where

$$B_1 = \cos(\varphi_1 + \theta_1(f) - 2\pi f\tau_0), \tag{10a}$$

$$C_1 = \sin(\varphi_1 + \theta_1(f) - 2\pi f\tau_0), \tag{10b}$$

$$B_2 = -\cos(\Delta p + \varphi_1 + \theta_2(f) - 2\pi f\tau_0), \tag{10c}$$

$$C_2 = -\sin(\Delta p + \varphi_1 + \theta_2(f) - 2\pi f\tau_0), \tag{10d}$$

finally, by using Equations (9) and (10), the magnitude of $S_{Rx}(t, f)$ is obtained as shown in Equation (11).

$$\begin{aligned} M_{Rx}(t,f) &= \sqrt{\begin{array}{l}\{A_1B_1a_1(f) + (\Delta m + A_1)B_2a_2(f)\}^2 \\ + \{A_1C_1a_1(f) + (\Delta m + A_1)C_2a_2(f)\}^2\end{array}} \\ &= \sqrt{\begin{array}{l}{A_1}^2{a_1}^2(f) + {a_2}^2(f)(\Delta m + A_1)^2 \\ -2A_1(\Delta m + A_1)a_1(f)a_2(f)\cos(\Delta p + \theta_2(f) - \theta_1(f))\end{array}}, \end{aligned} \tag{11}$$

as shown in Equation (11), the magnitude of the combined leakage signal $S_{Rx}(t, f)$ can be varied according to the phase and magnitude differences as well as the frequency response of two leakage signals. Therefore, all three leakage pairs in the proposed IBFD RF front-end should be simultaneously canceled out in order to achieve the high SIC. Using Equation (11), the SIC characteristic can be analyzed according to the conditions of *Tx* leakage signals in next sections.

2.1 | CASE 1: Two leakage signals are constant magnitude and phase with frequency

$S_{leak1}(t, f)$ and $S_{leak2}(t, f)$ are assumed to have constant magnitudes and phases along all frequencies ideally. Therefore, the frequency functions can be set as $a_1(f) = a_2(f) = 1$ and $\theta_1(f) = \theta_2(f) = 0$. Accordingly, the SIC for case 1 is written as Equation (12)

$$SIC_{case\,1} = \sqrt{\begin{array}{l}2{A_1}^2\{1-\cos(\Delta p)\} \\ +2A_1\Delta m\{1-\cos(\Delta p)\} + \Delta m^2\end{array}}, \tag{12}$$

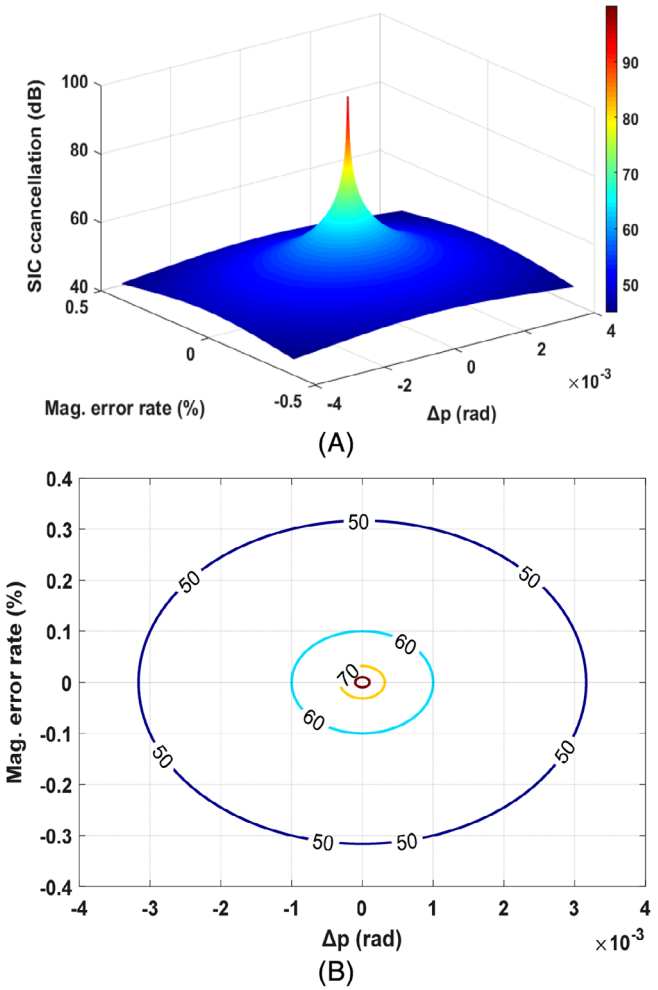

FIGURE 4 Self-interference cancellation (SIC) characteristics of case 1: A, SIC magnitude and B, SIC contours according to Δm and Δp

as shown in Equation (12), the SIC characteristic of the proposed IBFD RF front-end simply depends on Δm and Δp between the two constant signals. Figure 4 shows the SIC magnitude in dB scale using Equation (12) with normalized A_1 ($A_1 = 1$). The magnitude (Mag.) error rate is defined as a ratio of Δm to A_1 ($\Delta m/A_1 \times 100$). Figure 4A shows that the SIC magnitude is increased as Δm and Δp approach zero. Figure 4B shows the SIC contours in the range from 50 to 80 dB. For achieving more than 60 dB cancellation, the ranges of Δm and Δp must be within $\pm 0.1\%$ and $\pm 1 \times 10^{-3}$ (± 0.001) rad, respectively.

2.2 | CASE 2: Two leakage signals are frequency dependent magnitude and phase variations

In Case 1, the SIC is analyzed by assuming constant magnitude and phase of the leakage signals with respect to frequency. Therefore, case 1 cannot provide SIC bandwidth characteristics. To analyze SIC bandwidth, variation of magnitude and phase of leakages signals are defined with respect to frequency in case 2, which is similar to the practical case.

Figure 5 shows the magnitude and phase variations of leakage the signals that will use in the analysis. As shown this figure, the IBFD RF front-end has the most signal leakage characteristic at the center frequency ($f_0 = 1$), and the amount of leakage decreases as it moves away from the f_0. To consider frequency dependent variations

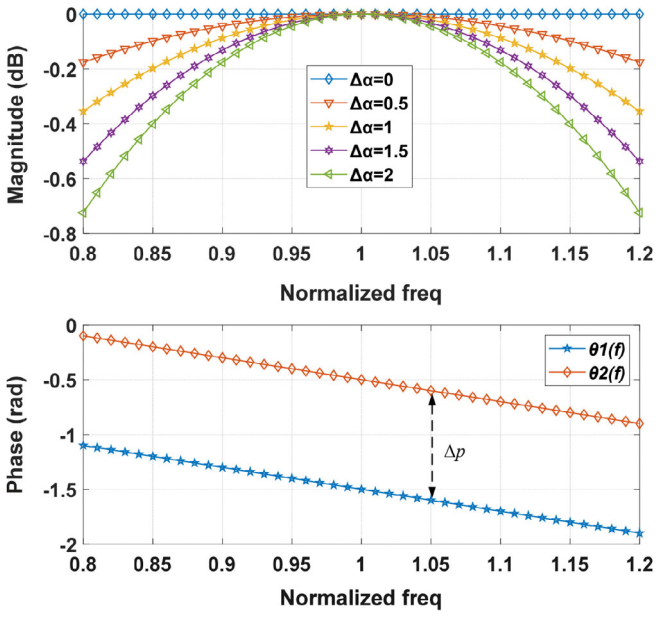

FIGURE 5 Magnitude and phase responses along with frequency in case 2

of leakage signals, $a_1(f)$ and $a_2(f)$ can be expressed as Equation (13)

$$a_1(f) = 1 - \frac{(f - f_0)^2}{f_0}, \tag{13a}$$

$$a_2(f) = 1 - \Delta\alpha \frac{(f - f_0)^2}{f_0}, \tag{13b}$$

Figure 5(A) shows the magnitude variation according to the magnitude slop coefficient ($\Delta\alpha$) and operating frequency variations of Equation (13b). The group delay can be expressed as the phase slope of the signal in the frequency domain. In the proposed IBFD RF front-end, the group delays of the two leakage signals are equal to τ_0 due to the physical balanced structure. Therefore, the phase slope of the two leakage signals should be the same. Accordingly, the phase variations $\theta_1(f)$ and $\theta_2(f)$ of the two leakage signals are the same and the phase difference between the two signals is expressed as Δp as shown in Figure 5. Using these conditions, the SIC be calculated as Equation (14) by using Equations (11) and (13).

$$SIC(t,f)_{case\,2} = \sqrt{\begin{array}{l} A_1{}^2 a_1{}^2(f) + a_2{}^2(f)(\Delta m + A_1)^2 - \\ 2A_1(\Delta m + A_1)a_1(f)a_2(f)\cos(\Delta p) \end{array}}. \tag{14}$$

Figure 6 shows the SIC magnitude of case 2 according to normalized frequencies and $\Delta\alpha$ using Equations (13) and (14). In order to observe the tendency of SIC according to $\Delta\alpha$, the other parameters (Δm and Δp) are set to zero, except for $A_1 = 1$. Figure 6A shows that the SIC magnitude is increased as $\Delta\alpha$ approaches one and the operating frequency approaches f_0 because the slope constant of $a_1(f)$ is one. Figure 6B shows the SIC contours according to $\Delta\alpha$ and normalized frequencies. It shows that the 60 dB SIC magnitude bandwidth is reduced according to increment and decrement of the $\Delta\alpha$ from one.

Figure 7 shows the calculated SIC magnitude with respect to normalized frequency, $\Delta\alpha$, and $\Delta p = 0.001$ rad. As shown in this figure, 60 dB SIC can be obtained with $\Delta p = 0.001$ rad, which exactly same case 1 if Δp is less than ± 0.001 rad. Figure 8 shows the calculated 60 dB SIC contours according to Δp variations with $\Delta m = 0$ and $A_1 = 1$. The color-filled regions inside the traces mean more than 60 dB SIC with respect to frequencies. The 60 dB SIC frequency bandwidths at $\Delta\alpha = 1.5$ are 0.93 to 1.07 (14%), 0.95 to 1.05 (10%), and 0.99 to 1.01 (2%) when Δp is 0, 0.0009, and 0.001 rad, respectively. It can observe that the 60 dB SIC bandwidth is decreased as Δp increases.

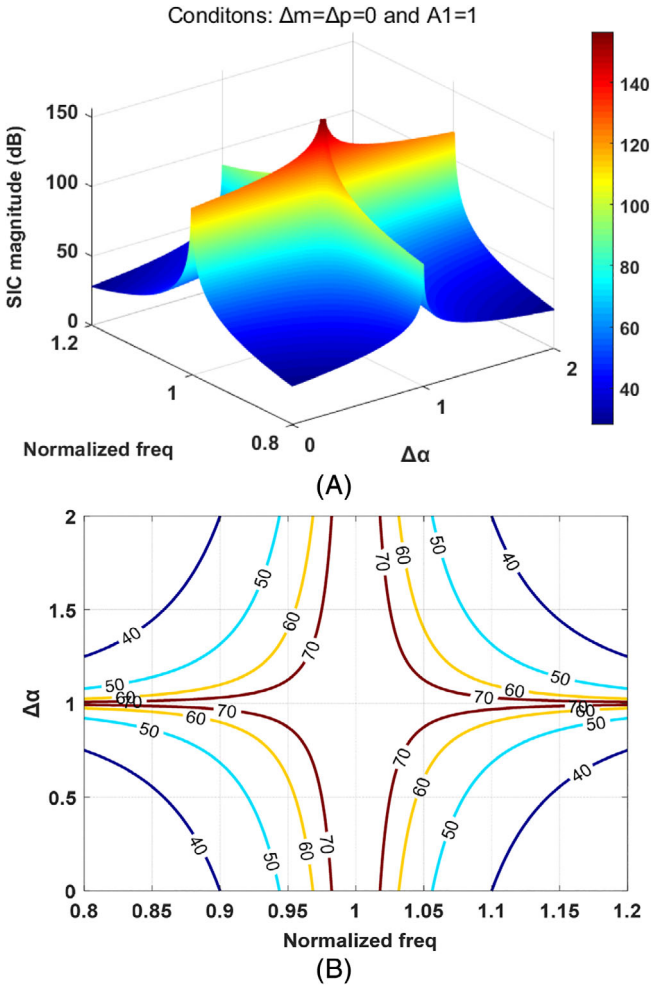

FIGURE 6 Self-interference cancellation (SIC) characteristics of case 2: A, SIC magnitude and B, SIC contours according to $\Delta\alpha$ and normalized frequencies

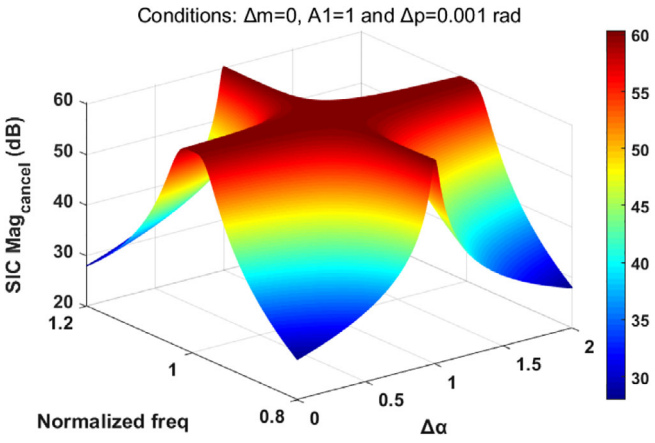

FIGURE 7 Self-interference cancellation (SIC) characteristics of case 2: SIC magnitude with $\Delta p = 0.001$ rad

The mathematical analysis shows that very precise adjustment of the cancellation signal is required to achieve 60 dB SIC. Therefore, the delicate design of the IBFD RF front-end is required. Also, antennas and their arrangements should be carefully selected because it affects the signal magnitude and phase variation in the operating band.

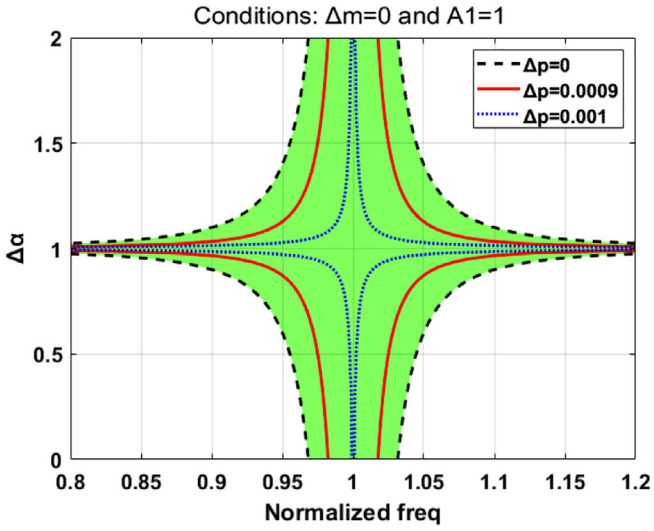

FIGURE 8 Self-interference cancellation (SIC) characteristics of case 2:60 dB SIC contours according to Δp

2.3 | Simulation and measurement results

2.3.1 | Out-of-phase balancing power splitter

In the previous section, the SIC characteristics were analyzed by assuming various conditions for leakage signal's magnitude and phase variations in case 1 and case 2. However, these assumptions do not show the practical frequency responses in the real operation. Still, these phenomena can provide the design tendencies of the proposed IBFD RF front-end. Therefore, the section compares the SIC simulation and measurement results using the actual magnitude and phase responses of 0°/180° power splitters.

The proposed magnetic-free IBFD RF front-end adopts out-of-phase BPS for high SIC between the Tx and Rx ports. Ring hybrid and Balun structures are generally used for 0°/180° power splitting. However, these structures cannot have broadband high SIC characteristics due to the narrow band out-of-phase and different τ characteristics which are caused by the different physical lengths in two power splitting paths. Therefore, the out-of-phase BPS structure is proposed to realize the equal magnitude, same τ, and out-of-phase transmission characteristics between two power splitting paths over a wide frequency bandwidth.

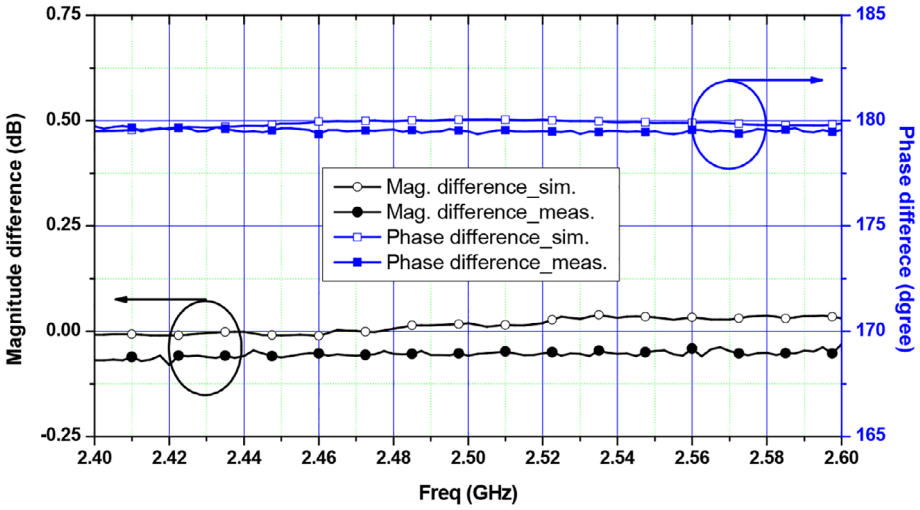

FIGURE 9 Magnitude and phase differences between the two output ports of out-of-phase balancing power splitter (BPS)

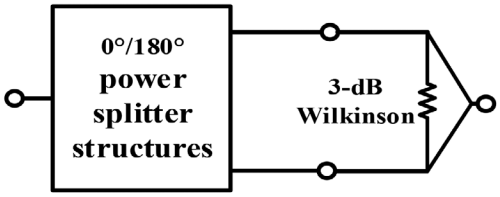

FIGURE 10 Block diagram of 0°/180° power splitter cancellation measurement

Figure 9 shows the magnitude and phase differences between the two output ports of out-of-phase BPS. Phase and magnitude differences are measured 179 ± 0.57° and 0.08 ± 0.0053 dB in 200 MHz bandwidth, respectively. Additionally, insertion loss and return losses at each port are measured 0.31 ± 0.02 dB at 2.5 GHz and more than 20 dB in 200 MHz bandwidth.

In order to verify the 0°/180° equal power division, the signal cancellation characteristics were simulated and measured by combining two output signals of 0°/180° power splitters with the Wilkinson power combiner, as shown in Figure 10. For simulation results, the magnitudes and phases of the two paths were extracted from measurement for the $a_1(f)$, $a_2(f)$, $\theta_1(f)$, and $\theta_2(f)$. Using these extracted data, SIC is calculated from Equation (11) using the MATLAB. These measured data were included in all the magnitude and phase information. Therefore, Δm and Δp are set at zero and A_1 is set at one.

Figure 11 shows a comparison of the signal cancellation characteristics among the proposed out-of-phase BPS, ring hybrid, and microstrip wideband Balun at 2.5 GHz.[24] The simulation and measurement results are consistent with each other. The proposed out-of-phase BPS shows the widest and highest SIC characteristics among all of the circuits. The ring hybrid shows high cancellation characteristics only in the narrowband because it has the 0°/180° phase splitting characteristic at the center frequency. Microstrip wideband Balun shows a relatively wider cancellation bandwidth than ring hybrid, but its cancellation is inferior to the proposed out-of-phase BPS. Therefore, the proposed out-of-phase BPS is considered suitable for implementation of the broadband SIC circuit.

2.3.2 | Magnetic-free IBFD RF front-end

In order to verify the proposed magnetic-free IBFD RF front-end, the IBFD RF front-end was implemented at 2.5 GHz WiMax frequency band. The proposed IBFD RF front-end was fabricated on an RT/Duriod 5880 substrate PCB obtained from Rogers, Inc. with a dielectric constant (ε_r) of 2.2 and thickness (h) of 31 mils. The used hybrid couplers is S03A2500N1 of ANAREN. As mentioned in the mathematical analysis, the return loss due to the impedance variation of the antenna can affect the SIC characteristics. To minimize this effect, the MAF94028 of Laird antenna with more than 15 dB return loss at the operating frequency was used.

Figure 12 shows a photograph of the fabricated magnetic-free IBFD RF front-end using out-of-phase BPS. The circuit size is 10×9 cm^2. Figure 13 shows the insertion loss of two Tx paths and the return losses at the Tx/Rx ports. As a measurement result, the insertion losses of both Tx paths are 3.337 ± 0.058 dB in the 200 MHz bandwidth. Considering the transmitted power of two Tx paths, the total insertion loss of the output is 0.34 dB at f_0, and all the Tx power is radiated by two Tx antennas. It shows that the proposed IBFD RF front-end removes the 3 dB insertion loss of the previous IBFD RF front-end circuits. Return losses at Tx and Rx ports are measured more than 18.7 dB in all 200 MHz bandwidth.

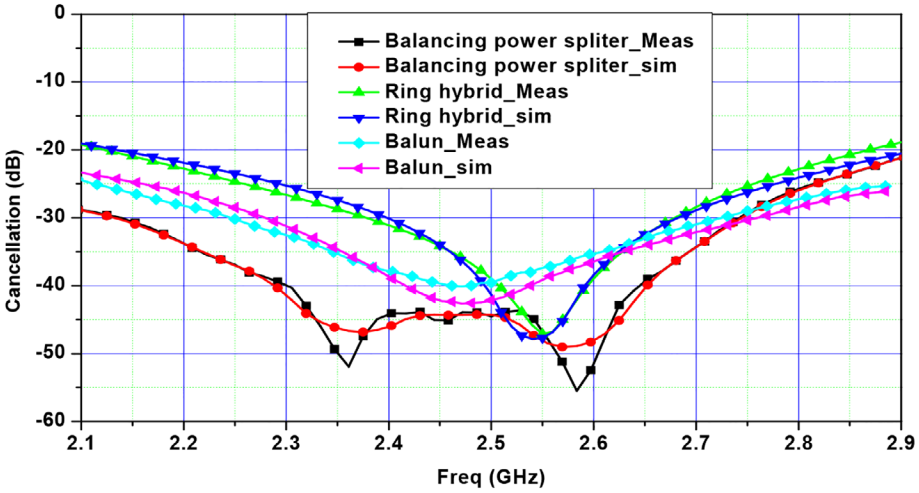

FIGURE 11 Signal cancellation comparison results among the 0°/180° power splitter structures

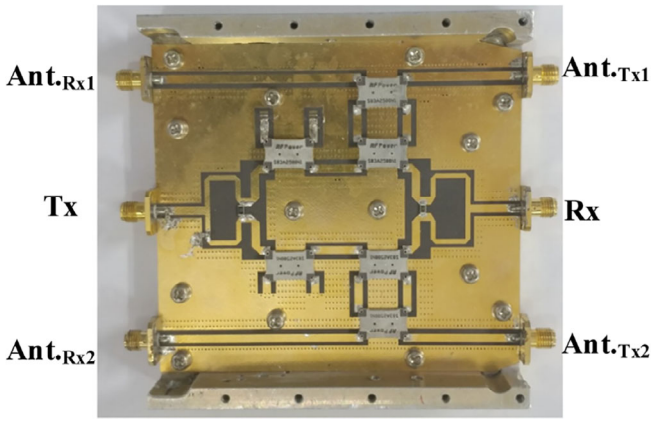

FIGURE 12 Photograph of the fabricated magnetic-free in-band full-duplex circuit

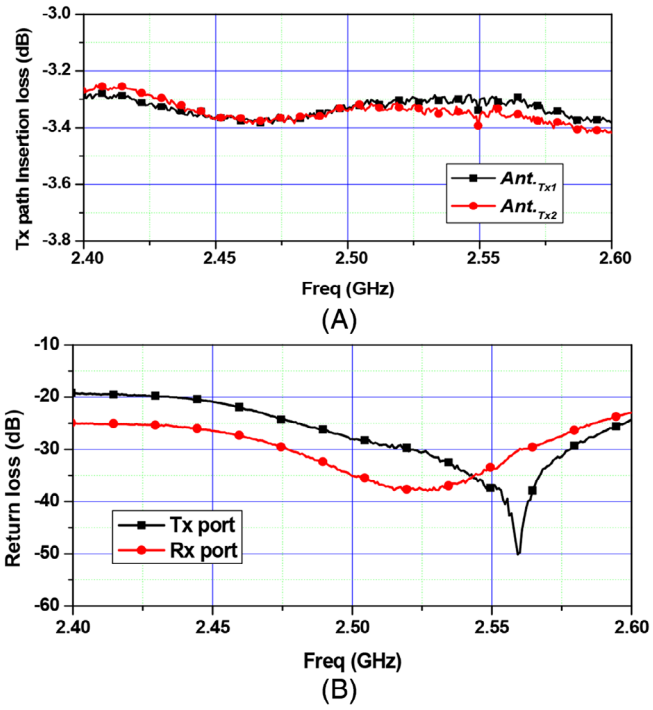

FIGURE 13 Measurement results of A, insertion losses at two transmitter (Tx) paths and B, return losses at Tx and receiver (Rx) ports

Figure 14 shows the noise figure measured on the Rx path. In the 200 MHz bandwidth, the noise figure is 0.6 ± 0.1 dB.

When multiple antennas are used, the SIC characteristics can be changed by the arrangement and distance of the antennas.[25] To obtain the high SIC by the minimizing cross-coupling among Tx and Rx antennas, the proposed circuit is used the antenna diversity technique. To take in account of effect of antenna arrangement, the SIC variations measured according to distance d with cross-shaped arrangement. Figure 15 shows the antenna setup block diagram used for SIC measurements. The proposed IBFD RF front-end uses two antennas each in Tx and Rx paths, respectively. Accordingly, the SIC characteristics can be changed due to the position and distance of the antennas. Tx and Rx antennas are arranged on the ± y-axis and the ± x-axis with distance d from the center, respectively.

Figure 16 shows the simulated radiation patterns of the dipole antennas using the high-frequency structure simulator of ANSYS. The maximum gains are 6.2, 5.1 and 4.1 dB when d is 15, 30 and 45 mm, respectively. Among the d variations, the maximum gain is obtained at d = 15 mm which is a quarter of wavelength distance between antennas at 2.5 GHz.

Figure 17 shows the measured Tx-to-Rx SIC characteristics of the proposed magnetic-free IBFD RF front-end according to the d. When the antenna ports are terminated at 50 Ω (without antennas), the 60 dB SIC bandwidths is 190 MHz (2.37-2.56 GHz). In the case of without antennas, there is no cross-coupling among the antennas, so only the first leakage pair signals are

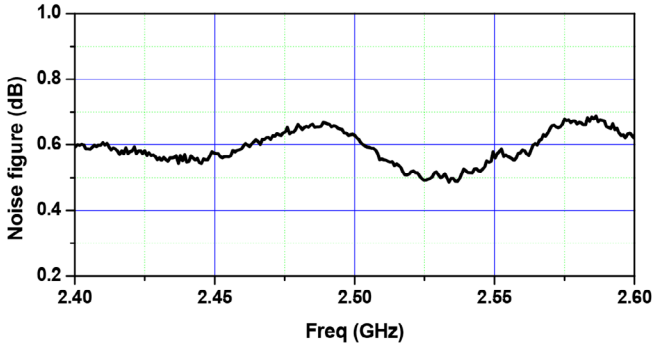

FIGURE 14 Measurement results of noise figure at receiver (Rx)

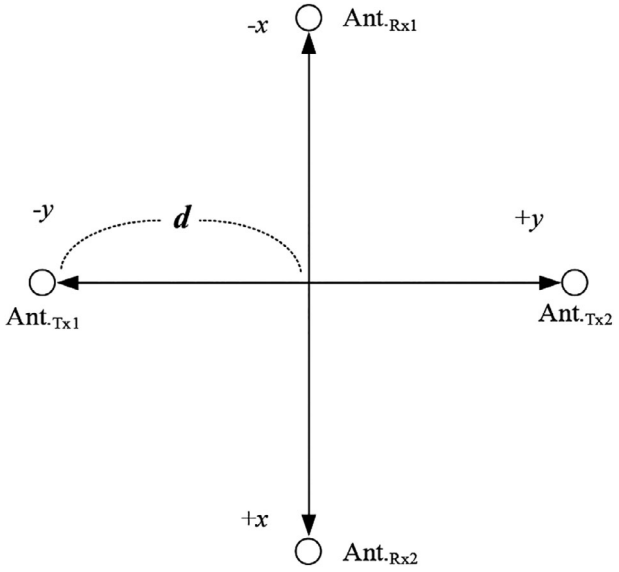

FIGURE 15 Block diagram of antennas setup for self-interference cancellation (SIC) measurement

cancelled out at the Rx port. Therefore, the SIC characteristic without antennas is better than SIC with antennas.

The 60 dB SIC bandwidths using four commercial dipole antennas are measured as 80 MHz (2.464-2.544 GHz) and 113 MHz (2.446-2.559 GHz) when d is 30 and 45 mm, respectively. When d is 15 mm, the amount of the coupling between the Tx and Rx antennas is large, therefore, 60 dB SIC characteristics cannot be obtained. The 50 dB SIC bandwidth and maximum SIC with d = 15 mm are 70 MHz (2.46-2.53 GHz) and 59.5 dB, respectively. The return loss characteristics of the proposed structure are changed due to the variation of the resonance characteristics of the antenna by d. Therefore, the return losses of the proposed structure are measured more than 12, 17 and 26.5 dB when d is 15, 30 and 45 mm, respectively. Table 2 shows a comparison of the electrical performances among the state-of-art

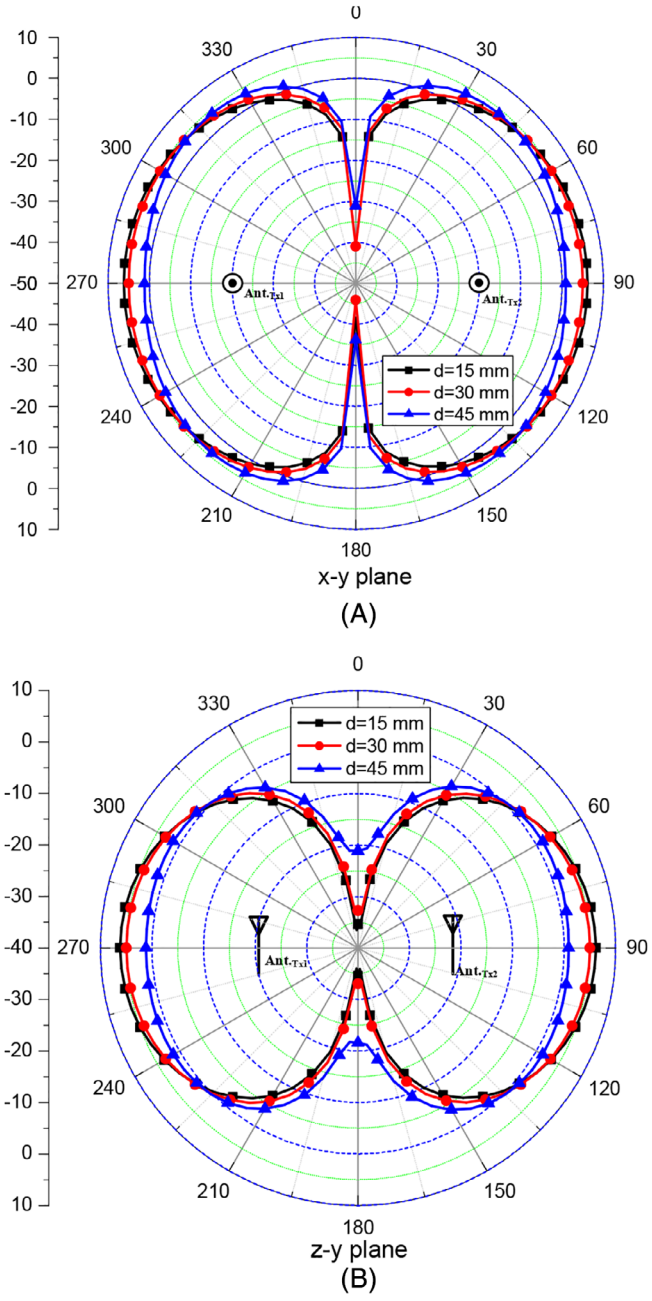

FIGURE 16 Simulation results of 2.5 GHz radiation patterns according to d: A, x-y plane and B, z-y plane

IBFD RF front-ends. The proposed magnetic-free IBFD RF front-end has the widest SIC bandwidth and the best SIC characteristic among the works using antennas and RF front-end SIC circuits.

3 | CONCLUSION

In this article, a design of magnetic-free IBFD RF front-end with antenna balancing structure is demonstrated. In order to realize the broadband SIC characteristics, the

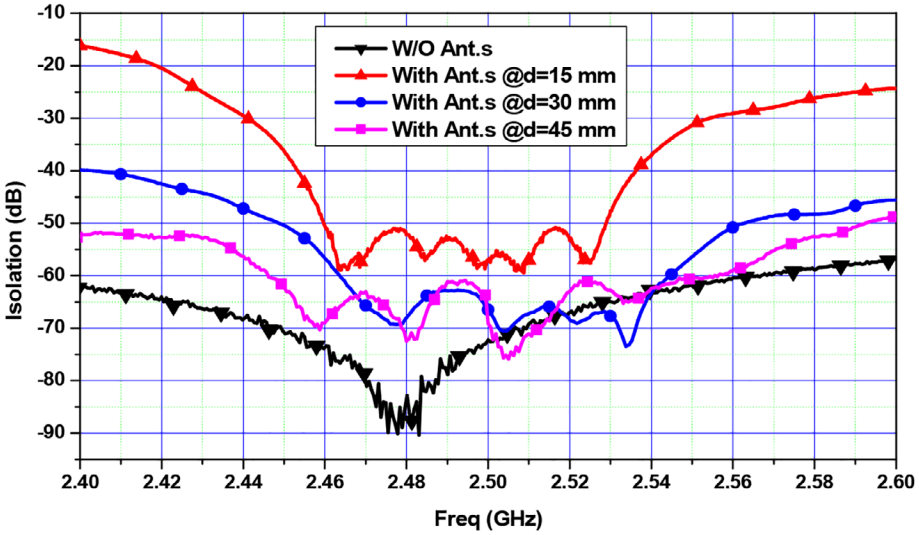

FIGURE 17 Measured self-interference cancellation (SIC) characteristics of proposed magnetic-free in-band full-duplex circuit according to *d*

TABLE 2 Electrical performances comparison with State-of-art IBFD RF front-ends

Ref.	f_0 [GHz]	SIC BW [MHz]	Return loss in SIC BW	FBW [%]	Magnetic device	Structure	Antenna
17	2.4	50 @ 60 dB	>10 dB	2.08	Magnetic-free	Antenna SIC	3-port patch antenna (1-*Tx* & 2-*Rx*)
18	4.6	300 @ 50 dB	>13 dB	6.52	Magnetic-free	Antenna SIC	2 patch antennas (1-*Tx* & 1- *Rx*)
26	0.914	26 @ 45 dB	non	2.84	Circulator	RF front-end SIC circuit	Dual-feed circularly polarized antenna (1-*Tx* & 1- *Rx*)
19	2.4	10 @ 45 dB	non	0.4	Magnetic-free	RF front-end SIC circuit	2 dipole antennas (1-*Tx* & 1- *Rx*)
21	2.5	80 @ 60 dB	non	3.2	Magnetic-free	RF front-end SIC circuit	3 dipole antennas (1-*Tx* & 2-*Rx*)
22	1.95	100 @ 52 dB	non	5.13	Circulator	RF front-end SIC circuit with balanced structure	2 dipole antennas (*Tx* & *Rx* common)
This work	2.5	210 @ 50 dB, $d = 45$ mm. 113 @ 60 dB, $d = 45$ mm	>19 dB	8.4. 4.52	Magnetic-free	RF front-end SIC circuit with balanced structure	4 dipole antennas (2-*Tx* & 2-*Rx*)

Abbreviation: IBDF, in-band full-duplex; Rx, receiver; SIC, self-interference cancellation; Tx, transmitter.

broadband out-of-phase BPS and balanced structure are proposed and verified. In the proposed structure, the SIC characteristics of the leakage signal pairs due to the balanced structure and cross-couplings among the antennas are described. Accordingly, the mathematical analysis with various leakage signal conditions is expressed to achieve consistent calculated cancellation performances with practical circuits.

The fabricated IBFD RF front-end characteristics are measured using commercial dipole antennas. The simulation and measurement results are consistent with each other. Based on the measurement results, the proposed magnetic-free IBFD RF front-end achieved 60 dB SIC characteristics over the wide frequency band and a better SIC characteristic than those of the conventional works. Moreover, the proposed magnetic-free IBFD is possible to implement and integrate in RF and microwave frequency bands. Therefore, the proposed circuit is suitable for implementing a broadband full-duplex system.

ACKNOWLEDGEMENT

This work was supported in part by the Korean Research Fellowship Program through the National Research Foundation (NRF) of Korea, in part the Ministry of

Science and ICT, under Grant 2016H1D3A1938065 and in part the National Research Foundation of Korea (NRF) grant funded by the Korea government (MSIT) (No. 2020R1A2C2012057).

DATA AVAILABILITY STATEMENT

Data available on request from the authors The data that support the findings of this study are available from the corresponding author upon reasonable request.

ORCID

Junhyung Jeong https://orcid.org/0000-0003-2383-1635
Girdhari Chaudhary https://orcid.org/0000-0003-2060-9860
Yongchae Jeong https://orcid.org/0000-0001-8778-5776

REFERENCES

1. D. Bharadia, E. McMilin, and S. Katti, Full duplex radios. Paper presented at: Proceedings of the ACM SIGCOMM, August, 2013.
2. Hong S, Brand J, Choi J, et al. Application of self-interference cancellation in 5G and beyond. *IEEE Commun Mag*. 2014;52(2):114-121.
3. Reiskarimian N, Zhou J, Krishnaswamy H. A CMOS passive LPTV non-magnetic circulator and its application in a full-duplex receiver. *IEEE J Solid-State Circuits*. 2017;52(5):1358-1372.
4. Zhang L, Krishnaswamy H. Arbitrary analog/RF spatial filtering in digital MIMO receiver arrays. *IEEE J. Solid-State Circuits*. 2017;52(12):3392-3404.
5. D. Korpi, M. AghababaeeTafreshi, M. Piilila, L. Anttila, and M. Valkama. Advanced architectures for self-interference cancellation in full-duplex radios: algorithms and measurements. Paper presented at: Proceedings of the 50th Asilomar Conference on Signals, Systems and Computers, November, 2016.
6. T. Chen, J. Zhou, N. Grimwood, R. Fogel, J. Marašević, H. Krishnaswamy, and G. Zussman, Full-duplex wireless based on a small-form-factor analog self-interference canceller. Paper presented at: Proceedings of the 17th ACM International Symposium Mobile Ad Hoc Networking and Computing, July 2016.
7. H. Hamazumi, K. Imamura, N. Iai, K. Shibuya, and M. Sasaki, A study of a loop interference canceller for the relay stations in an SFN for digital terrestrial broadcasting. Paper presented at: Proceedings of the IEEE Global Communications Conference, November, 2000.
8. B. Chun, E. Jeong, J. Joung, Y. Oh, and Y. H. Lee, Pre-nulling for self-interference suppression in full-duplex relays. Paper presented at: Proceedings of the Asia-Pacific Signal and Information Processing Association Annual Summit Conference, October, 2009.
9. Ju H, Oh E, Hong D. Improving efficiency of resource usage in two-hop full duplex relay systems based on resource sharing and interference cancellation. *IEEE Trans Wirel Commun*. 2009;8(8):3933-3938.
10. Riihonen T, Werner S, Wichman R. Mitigation of loopback self-interference in full-duplex MIMO relays. *IEEE Trans Signal Process*. 2011;59(12):5983-5993.
11. Laughlin L, Beach MA, Morris KA, Haine JL. Electrical balance duplexing for small form factor realization of in-band full duplex. *IEEE Commun Mag*. 2015;53(5):102-110.
12. L. Laughlin, C. Zhang, M. A. Beach, K. A. Morris, and J. Haine, A widely tunable full duplex transceiver combining electrical balance isolation and active analog cancellation. Paper presented at: IEEE Vehicular Technology Conference, May, 2015.
13. Kumar A, Aniruddhan S. A 2.5-GHz CMOS full-duplex front-end for asymmetric data networks. *IEEE Trans Circuits Syst I, Reg Papers*. 2018;65(10):3174-3185.
14. Sayed AE, Mishra AK, Ahmed AH, et al. A Hilbert transform equalizer enabling 80 MHz RF self-interference cancellation for full-duplex receivers. *IEEE Trans. Circuits Syst. I, Reg. Papers*. 2019;66(3):1153-1165.
15. Chaudhuri S, Kshetrimayum RS, Sonkar RK. High inter-port isolation dual circularly polarized slot antenna with interdigital capacitor. *Int J RF Microw Comput Aided Eng*. 2019;29(10). https://doi.org/10.1002/mmce.21903.
16. Nawaz H, Ahmad U. A compact proximity-fed 2.4 GHz monostatic antenna with wide-band SIC characteristics for in-band full duplex applications. *Int J RF Microw Comput Aided Eng*. 2020;30(3). https://doi.org/10.1002/mmce.22087.
17. Nawaz H, Tekin I. Dual-polarized, differential fed microstrip patch antennas with very high interport isolation for full duplex communication. *IEEE Trans Antennas Propag*. 2017;65(12):7355-7360.
18. T. Dinc and H. Krishnaswamy. A T/R antenna pair with polarization-based reconfigurable wideband self-interference cancellation for simultaneous transmit and receive. Paper presented at: Proceedings of the IEEE International Microwave Symposium, July, 2015.
19. M. Jain, J. Choi, T. Kim, D. Bharadia, K. Srinivasan, S. Seth, P. Levis, S. Katti, and P. Sinha, Practical, real-time, full duplex wireless. Paper presented at: Proceedings of the 17th Annual International Conference Mobile Computer Network, September, 2011.
20. Laughlin L, Beach MA, Morris KA, Haine JL. Optimum single antenna full duplex using hybrid junctions. *IEEE J Sel Area Commun*. 2014;32(9):1653-1661.
21. D. Lee and B. Min, 1-TX and 2-RX in-band full-duplex readio front-end with 60 dB self-interference cancellation. Paper presented at: Proceedings of the IEEE International Microwave Symposium, May 2015
22. Tang A, Wang X. Balanced RF-circuit based self-interference cancellation for full duplex communications. *J Ad Hoc Netw*. 2015;24:214-227.
23. Ahn H-R. *Asymmetric Passive Components in Microwave Integrated Circuits*. Hoboken, NJ, USA: Wiley; 2006.
24. Q. Wang, H. Kang, S. Jeong, J, Jeong, P. Kim, and Y. Jeong, Analysis and design of conventional wideband branch line balun. Paper presented at: Proceedings of the International Symposium on Information Technology Convergence, October, 2015.
25. E. Aryafar, M. Khojastepour, K. Sundaresan, S. Rangarajan, and M. Chiang, MIDU: enabling MIMO full duplex. Paper presented at: Proceedings of the18th Annual International Conference on Mobile Computing and Networking, August, 2012

26. M. E. Knox, Single antenna full duplex communications using a common carrier. Paper presented at: Proceedings of the IEEE Wireless & Microwave Technology Conference, April, 2012.

AUTHOR BIOGRAPHIES

Junhyung Jeong (S'13) received the B.E. degree in electronics & information engineering from the Jeonbuk national university, Jollabuk-do, Republic of Korea, in 2012, the M.E. degree in electronics engineering from the Jeonbuk National University, Jollabuk-do, Republic of Korea, in 2014 and PhD degree in electronics engineering from Jeonbuk National University, Republic of Korea in 2020. He is currently working as Post-Doc at the Korea Electronics Technology Institute (KETI), Jeonju, South Korea. His research interests include RF filter, high-efficiency power amplifiers, antenna, EMC and RF transmitter.

Girdhari Chaudhary (S'10-M'13) received the B.E. and M. Tech. degrees in Electronics and Communication Engineering from Nepal Engineering College (NEC), Kathmandu, Nepal and MNIT, Jaipur, India in 2004 and 2007, respectively and PhD degree in Electronics Engineering from Jeonbuk National University, Republic of Korea in 2013. He is currently working as Assistant Research Professor at Division of Electronics Engineering, Jeonbuk National University, Korea. He worked as Principal Investigator (PI) of independent Project through Basic Science Research Program of the National Research Foundation (NRF) of funded by the Ministry of Education Korea. He is also recipient of the BK21 PLUS Research Excellence Award 2015 from the Ministry of Education, Republic of Korea. Currently, he has received Korean Research Fellowship (KRF) through the National Research Foundation (NRF) of Korea funded by the Ministry of Science and ICT. His research interests include multi-band tunable passive circuits, negative group delay circuits and its applications, in-band full duplex systems and high efficiency power amplifiers. Dr. Chaudhary has served as reviewer of IEEE Transaction on Microwave Theory and Techniques, IEEE Microwave and Wireless Component Letters, IEEE Transaction on Circuit and Systems-I, and IEEE Transaction on Industrial Electronics.

Yongchae Jeong (M'99-SM'10) received BSEE and MSEE, and Ph.D. degrees in electronics engineering from Sogang University, Seoul, Republic of Korea in 1989, 1991, and 1996, respectively. From 1991 to 1998, he worked as a senior engineer with Samsung Electronics. From 1998, he joined Division of Electronics Engineering, Jeonbuk National University, Jeonju, Republic of Korea. From July 2006 to December 2007, he joined at Georgia Institute of Technology as a visiting Professor. Now, he is a professor, member of IT Convergence Research Center, and director of HOPE-IT Human Resource Development Center of BK21 PLUS in Jeonbuk National University. He is currently teaching and conducting research in the area of microwave passive and active circuits, mobile and satellite base-station RF system, design of periodic defected transmission line, negative group delay circuits and its applications, in-band full duplex radio and RFIC design. Prof. Jeong is a senior member of IEEE and member of KIEES (Korea Institute of Electromagnetic Engineering and Science). He has authored and co-authored over 200 papers in international journals and conference proceeding.

How to cite this article: Jeong J, Chaudhary G, Jeong Y. A magnetic-free in-band full-duplex RF front-end with antenna balancing structure. *Int J RF Microw Comput Aided Eng*. 2021;31:e22623. https://doi.org/10.1002/mmce.22623